IEEE Access
Multidisciplinary ⋮ Rapid Review ⋮ Open Access Journal

Received January 23, 2018, accepted February 19, 2018, date of publication February 27, 2018, date of current version March 15, 2018.

Digital Object Identifier 10.1109/ACCESS.2018.2809918

Series-, Parallel-, and Inter-Connection of Solid-State Arbitrary Fractional-Order Capacitors: Theoretical Study and Experimental Verification

ASLIHAN KARTCI[1,2], (Student Member, IEEE), AGAMYRAT AGAMBAYEV[3], (Student Member, IEEE), NORBERT HERENCSAR[2], (Senior Member, IEEE), AND KHALED N. SALAMA[3], (Senior Member, IEEE)

[1]Department of Radio Electronics, Brno University of Technology, 616 00 Brno, Czech Republic
[2]Department of Telecommunications, Brno University of Technology, 616 00 Brno, Czech Republic
[3]Computer, Electrical and Mathematical Sciences and Engineering Division, King Abdullah University of Science and Technology, Thuwal 23955, Saudi Arabia

Corresponding author: Aslihan Kartci (kartci@feec.vutbr.cz)

This work was supported in part by COST Action CA15225, a network supported by COST (European Cooperation in Science and Technology), in part by the National Sustainability Program under Grant LO1401, and in part by the Czech Science Foundation under Grant 16-06175S. For the research, infrastructure of the SIX Center was used.

ABSTRACT In this paper, general analytical formulas are introduced for the determination of equivalent impedance, magnitude, and phase, i.e., order, for n arbitrary fractional-order capacitors (FoCs) connected in series, parallel, and their interconnection. The approach presented helps to evaluate these relevant quantities in the fractional domain, since the order of each element has a significant effect on the impedance of each FoC and their equivalent capacitance cannot be considered. Three types of solid-state fractional-order passive capacitors of different orders, using ferroelectric polymer and reduced graphene oxide-percolated P(VDF-TrFE-CFE) composite structures, are fabricated and characterized. Using an impedance analyzer, the behavior of the devices was found to be stable in the frequency range $0.2 - 20$ MHz, with a phase angle deviation of $\pm 4°$. Multiple numerical and experimental case studies are given, in particular for two and three connected FoCs. The fundamental issues of the measurement units of the FoCs connected in series and parallel are derived. A MATLAB open-access source code is given in the Appendix for easy calculation of the equivalent FoC magnitude and phase. The experimental results are in good agreement with the theoretical assumptions.

INDEX TERMS Arbitrary-order FoC, FoC, fractional calculus, fractional-order capacitor, interconnection, MATLAB open access source code, parallel connection, series connection, solid-state device.

I. INTRODUCTION

Fractional-(non-integer)-order circuits and systems offer unique benefits by enabling broader impedance matching and allowing the tunability of frequency response of electronic circuits. So-called fractional-order capacitors (FoCs), known also as constant-phase elements, are crucial fundamental components of these circuits and are extensively used in a wide range of applications [1]–[26]. As is known, FoCs possess both real and imaginary impedance components since the fractional models need to account for both the order and frequency, while an ideal capacitor has only an imaginary component. In electrical engineering in particular, the constant-phase behavior of capacitors is explained as the frequency dispersion of the capacitance by dielectric relaxation, where the electric current density follows changes in the electric field with a delay. In 1994, to express this phenomenon of ''off the shelf'' real capacitors mathematically, the capacitance current in the time domain was given as [27]:

$$i(t) = C\frac{d^{\alpha}u(t)}{dt^{\alpha}}, \quad 0 < \alpha < 1, \tag{1}$$

where $d^{\alpha}u(t)/dt^{\alpha}$ denotes the 'fractional-order time derivative'. Now, the impedance of an ideal FoC can be derived from

(1) in the frequency domain as:

$$Z(s) = Ds^{-\alpha}. \quad (2)$$

Here, α is the order of the FoC, which is known as the dispersion coefficient, and D is the coefficient of pseudo-capacitance expressed in units of Farad·sec$^{\alpha-1}$. By substituting $j\omega$ for s, where j is a complex number and ω is the radial frequency, in the frequency domain the impedance becomes:

$$|Z(j\omega)| = \left|D(j\omega)^{-\alpha}\right| = \left|D\omega^{-\alpha}\left(\cos\varphi + j\sin\varphi\right)\right|, \quad (3)$$

where the phase is given in radians ($\varphi = -\alpha\pi/2$) or in degrees [°] ($\varphi = -90\alpha$), while the argument in ohms [Ω]. Accordingly, the magnitude depends on frequency versus α and its value varies by 20α dB per decade of frequency and its characteristic decreases. However, the argument φ of the impedance is constant and independent of the angular frequency ω.

The series and parallel connections of FoCs are the two elementary and most important structures that allow us to calculate the impedance of equivalent capacitance. They play a crucial role in investigating the dielectric properties of zinc flakes/flexible polyvinylidene fluoride (ZFs/PVDF) composites [28] and in practical applications such as modelling of supercapacitors [29] or designing of supercapacitor banks [30]. Since the order of each element in the connection has a significant effect on the impedance of each FoC, it cannot be neglected when calculating equivalent impedance. Bearing these ideas in mind, to the best of the authors' knowledge, there are only a few studies that focus on the series and parallel connection of FoCs, mainly on the theoretical level only [31]–[34]. In [31], the equivalent impedance expressions of identical-order FoCs connected in series and parallel are given, but they were not proved by experiments due to lack of commercially available FoCs. Recently, the equivalent magnitude and phase formulas of two identical-order FoCs connected in series and in parallel have been verified experimentally by integrated operational transconductance amplifier (OTA)-based emulators [32]. Later on, in [33] and [34], Pu showed the possibility of connections between arbitrary orders of fractals. However, the theory that Pu introduced is based on positioning the purely ideal fractor in Chua's circuit axiomatic element system and is not sufficient to calculate the equivalent magnitude and phase, i.e. order of FoCs, easily. Therefore, the main contributions of the present work are:

1) The general formulas for impedance, magnitude, and phase response of the series and parallel arbitrary-order n FoCs according to the main definition of the FoC are given as a complete study. Furthermore, the units of these physical dimensions are discussed.
2) Three types of fabricated ferroelectric polymer or reduced Graphene Oxide (rGO)-percolated P(VDF-TrFE-CFE) composite structure-based passive FoC devices of three different orders are described, together with their precise characterization including their pseudo-capacitances and bandwidth of operation. Note that this paper reports the first experimental verification of series- and parallel-connected FoCs by fabricated solid-state passive FoCs, in contrast to using RC ladder structures [31] or active IC emulators [32].
3) Theoretical assumptions calculated via a newly developed MATLAB open access source code given in Appendix are proved by experimental verification using fabricated passive FoCs. Here it is important to underline that although the integer-order case (identical orders $\alpha = 1$) is well-known as the core of the physical calculation, the fractional-order (arbitrary-orders) as a novel case also matches well with the assumptions and proves our novel core idea.

The rest of the paper is organized as follows: In Section II, the general formulas for impedance, magnitude, and phase responses of series- and parallel-connected n FoCs are derived. Fabrication process and experimental characterization of three types (orders 0.69 (TP2), 0.92 (P2), 0.62 (G2)) of solid-state compact and stable-in-phase (in the measured frequency range 0.2 MHz − 20 MHz) electric passive FoCs, in particular those based on an actual dielectric material, are explained in Section III A. The experimental results for two and three series-, parallel-, and inter-connected FoCs are presented in Section III B. A brief discussion of obtained results and final conclusions are given in Sections IV and V, respectively.

II. MATHEMATICAL DESCRIPTION OF n FoCs CONNECTION

This section aims to introduce general formulas that help to simplify n FoCs connected in a circuit. Hence, based on the proposed fractional-order measurement units and physical dimensions of FoC, the rules for in-series and parallel connected FoCs are presented.

A. ANALYSIS OF FRACTIONAL-ORDER CAPACITORS IN SERIES

In particular, having multiple FoCs in a circuit, the main aim is to replace them with a single equivalent capacitor and/or reach a desired phase angle with a combination of arbitrary-order capacitors. Therefore, considering the connection of n FoCs in series as shown in Fig. 1, the impedance of each FoC can be described as: $Z_{\alpha_1}(s) = \frac{1}{s^{\alpha_1}C_{\alpha_1}}$, $Z_{\alpha_2}(s) = \frac{1}{s^{\alpha_2}C_{\alpha_2}}$, $Z_{\alpha_3}(s) = \frac{1}{s^{\alpha_3}C_{\alpha_3}}$, …, $Z_{\alpha_n}(s) = \frac{1}{s^{\alpha_n}C_{\alpha_n}}$. Assuming the voltage across it is $v_{\alpha_1} + v_{\alpha_2} + v_{\alpha_3} + \ldots + v_{\alpha_n} = v_{\text{eq,s}}$ and the current flowing through is $i_{\alpha_1} = i_{\alpha_2} = i_{\alpha_3} = \ldots = i_{\alpha_n} = i_{\text{eq,s}}$, the equivalent total impedance $Z_{\text{eq,s}}$, and its unit is

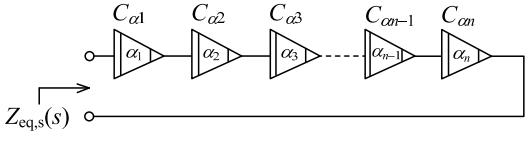

FIGURE 1. Series-connection of n FoCs.

derived as:

$$Z_{\text{eq,s}}(s) = Z_{\alpha_1} + Z_{\alpha_2} + Z_{\alpha_3} + \ldots + Z_{\alpha_n} = \sum_{i=1}^{n} \frac{1}{s^{\alpha_i} C_{\alpha_i}}. \ [\Omega] \tag{4}$$

By using Euler's identity $s = j\omega$, while $j = e^{j\pi/2}$, and substituting in (4), the general formulas for equivalent magnitude and phase responses of n FoCs connected in series are expressed as (5) and (6), respectively, where the indexes from i to k are the numbers of FoCs, each counted from 1 to n. The function of the sum is valid under the condition that $i < j < \ldots < l$ and $k \neq i, j, \ldots, l$. Note that the derived orders of FoCs affect the power of angular frequency and also the degree of the cosine in magnitude function (5). Furthermore, the phase of the equivalent FoC is dependent on the angular frequency ω. From (6) it is evident that the angle with the positive x-axis is decreasing while the sum of orders is increasing. The phase of FoC must be between $0 < \text{Arg}[Z_{\text{eq,s}}(s)] < -\pi/2$.

Now, let us consider Case I, when FoCs have different pseudo-capacitances, i.e. $C_{\alpha_1} \neq C_{\alpha_2} \neq C_{\alpha_3} \neq \ldots \neq C_{\alpha_n}$, while assuming their orders are identical $\alpha_1 = \alpha_2 = \alpha_3 = \ldots = \alpha_n = \alpha$ ($\alpha \in (0, 1]$). Then the impedance, magnitude, and phase formulas in (4)–(6) turn out to be as given in Table 1, where in (7) and (8) $\sum_{i=1}^{n} \frac{1}{C_{\alpha_i}} = \frac{1}{C_{\text{eq,s}}}$. The given case study is straightforward since each capacitor will be experiencing the same current and the voltage across each FoC will increase with respect to this current. Thus, the total voltage across all capacitors will increase at a greater rate than the voltage across individual capacitors.

On the other hand, in Case II, when considering the same pseudo-capacitances of FoCs, i.e. assuming $C_{\alpha_1} = C_{\alpha_2} = C_{\alpha_3} = \ldots = C_{\alpha_n} = C_\alpha$ with identical orders, the impedance, magnitude, and phase in (4)–(6) respectively become (10)–(12) of Table 1. From (12) it is clear that the phase is independent of angular frequency and number of capacitances, while the magnitude is dependent on both these values. However, the order of capacitors affects all responses. In other words, FoCs follow the same rule as integer-order capacitors when combined in series only if they have both identical pseudo-capacitances and equal orders. From (9) and (12), the order of an equivalent FoC can be easily calculated from $\alpha = -2\text{Arg}[Z_{\text{eq,s}}(s)]/\pi$.

TABLE 1. Case studies of series-connected FoCs in (4)–(6).

$Z_{\text{eq,s}}(s)$ [Ω]	$\lvert Z_{\text{eq,s}}(s)\rvert$ [Ω]	Arg$[Z_{\text{eq,s}}(s)]$ [Degree]
Case I: $C_{\alpha_1} \neq C_{\alpha_2} \neq C_{\alpha_3} \neq \ldots \neq C_{\alpha_n}$ with identical order α		
$\frac{1}{s^\alpha}\left(\sum_{i=1}^{n}\frac{1}{C_{\alpha_i}}\right)$ (7)	$\frac{1}{\omega^\alpha}\left(\sum_{i=1}^{n}\frac{1}{C_{\alpha_i}}\right)$ (8)	$-\alpha\frac{\pi}{2}$ (9)
Case II: $C_{\alpha_1} = C_{\alpha_2} = C_{\alpha_3} = \ldots = C_{\alpha_n} = C_\alpha$ with identical order α		
$\frac{n}{s^\alpha C_\alpha}$ (10)	$\frac{n}{\omega^\alpha C_\alpha}$ (11)	$-\alpha\frac{\pi}{2}$ (12)

B. ANALYSIS OF FRACTIONAL-ORDER CAPACITORS IN PARALLEL

When n FoCs with arbitrary order are connected in parallel as shown in Fig. 2, the goal is again to replace them with a single equivalent FoC.

According to Kirchhoff's Voltage Law, the voltage across

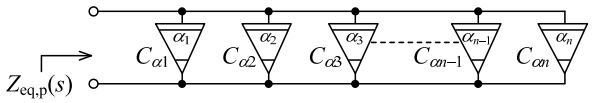

FIGURE 2. Parallel-connection of n FoCs.

$$\left|Z_{\text{eq,s}}(s)\right| = \frac{\sqrt{\sum\limits_{\substack{i,j,\ldots,l,k=1\\ i<j<\ldots<l\\ k\neq i,j,\ldots,l}}^{n} \omega^{2(\alpha_i+\alpha_j+\ldots+\alpha_l)} \frac{1}{C_{\alpha_k}^2} + 2\left\{\sum\limits_{\substack{i,j,\ldots,l,k=1\\ i<j<\ldots<l\\ k\neq i,j,\ldots,l}}^{n} \omega^{(\alpha_i+\alpha_j+\ldots+\alpha_l+2\alpha_k)} \cos\left[(\alpha_i-\alpha_j)\frac{\pi}{2}\right]\right\}}}{\prod\limits_{i=1}^{n}\omega^{\alpha_i}}, \quad [\Omega] \tag{5}$$

$$\text{Arg}\left[Z_{\text{eq,s}}(s)\right] = \tan^{-1}\left\{\frac{\sum\limits_{\substack{i,j,\ldots,l,k=1\\ i<j<\ldots<l\\ k\neq i,j,\ldots,l}}^{n} \omega^{(\alpha_i+\alpha_j+\ldots+\alpha_l)} \frac{1}{C_{\alpha_k}} \sin\left[\left(\alpha_i+\alpha_j+\ldots+\alpha_l\right)\frac{\pi}{2}\right]}{\sum\limits_{\substack{i,j,\ldots,l,k=1\\ i<j<\ldots<l\\ k\neq i,j,\ldots,l}}^{n} \omega^{(\alpha_i+\alpha_j+\ldots+\alpha_l)} \frac{1}{C_{\alpha_k}} \cos\left[\left(\alpha_i+\alpha_j+\ldots+\alpha_l\right)\frac{\pi}{2}\right]}\right\} - \sum_{i=1}^{n}(\alpha_i)\frac{\pi}{2}, \quad [\text{Degree}] \tag{6}$$

each capacitor must be the same and let us label it as $v_{\text{eq,p}}$. In addition, applying Kirchhoff's Current Law, the sum of currents in nodes will be $i + i_{\alpha_1} + i_{\alpha_2} + i_{\alpha_3} + \ldots + i_{\alpha_n} = i_{\text{eq,p}}$. Hence, by substituting the current flowing through each capacitor in the time-domain and transforming it to the Laplace domain, the equivalent total impedance $Z_{\text{eq,p}}$ of n arbitrary-order FoCs connected in parallel can be expressed as:

$$\frac{1}{Z_{\text{eq,p}}(s)} = \frac{1}{Z_{\alpha_1}} + \frac{1}{Z_{\alpha_2}} + \frac{1}{Z_{\alpha_3}} + \ldots + \frac{1}{Z_{\alpha_n}}, \tag{13}$$

$$Z_{\text{eq,p}}(s) = \frac{1}{s^{\alpha_1}C_{\alpha_1} + s^{\alpha_2}C_{\alpha_2} + s^{\alpha_3}C_{\alpha_3} + \ldots + s^{\alpha_n}C_{\alpha_n}} = \frac{1}{\sum_{i=1}^{n} s^{\alpha_i}C_{\alpha_i}}. \ [\Omega] \tag{14}$$

Thus, by substituting in (14) $s = j\omega$, while $j = e^{j\pi/2}$, the expressions for magnitude and phase are as follows:

$$\left|Z_{\text{eq,p}}(s)\right| = \frac{1}{\sqrt{\sum_{i=1}^{n}\omega^{2\alpha_i}C_{\alpha_i}^2 + 2\left[\sum_{\substack{i,j=1\\ i<j}}^{n}\omega^{\alpha_i+\alpha_j}C_{\alpha_i}C_{\alpha_j}\cos(\alpha_i-\alpha_j)\frac{\pi}{2}\right]}}, \ [\Omega] \tag{15}$$

$$\text{Arg}\left[Z_{\text{eq,p}}(s)\right] = -\tan^{-1}\left[\frac{\sum_{i=1}^{n}\omega^{\alpha_i}C_{\alpha_i}\sin\left(\alpha_i\frac{\pi}{2}\right)}{\sum_{i=1}^{n}\omega^{\alpha_i}C_{\alpha_i}\cos\left(\alpha_i\frac{\pi}{2}\right)}\right]. \ [\text{Degree}] \tag{16}$$

Again, when considering Case III, where FoCs have identical orders $\alpha_1 = \alpha_2 = \alpha_3 = \ldots = \alpha_n = \alpha$ ($\alpha \in (0, 1]$) but different pseudo-capacitances, i.e. $C_{\alpha_1} \neq C_{\alpha_2} \neq C_{\alpha_3} \neq \ldots \neq C_{\alpha_n}$, then the impedance, magnitude, and phase responses are derived as (17)–(19) of Table 2, where in (17) and (18) $\sum_{i=1}^{n} C_{\alpha_i} = C_{\text{eq,p}}$. On the other hand (Case IV), if $\alpha_1 = \alpha_2 = \alpha_3 = \ldots = \alpha_n = \alpha$ ($\alpha \in (0, 1]$) and $C_{\alpha_1} = C_{\alpha_2} = C_{\alpha_3} = \ldots = C_{\alpha_n} = C_\alpha$, then (17)–(19) turn out to be (20)–(22).

Similar to Cases I and II of the arbitrary FoCs connected in series, the equivalent order of the resulting network is frequency-dependent and given by (16), but if the orders are identical, then it is frequency-independent as shown in (19) and (22) of Table 2. However, when n identical-order FoCs are connected in parallel, the total equivalent impedance, magnitude, and phase responses are as simple as (20)–(22). It is worth noting that these relations are similar to integer-order capacitors connected in parallel. Hence, by increasing the number of capacitors, the equivalent magnitude may decrease and equivalent pseudo-capacitance may increase. In addition, the frequency and number of capacitors influence only the magnitude, while the order affects both the magnitude and phase responses. Units of impedance, magnitude, and phase responses of FoCs remain in both the series and parallel cases the same as in the integer-order case, i.e. the impedance and magnitude are in units of ohms and the phase in units of degrees, respectively.

TABLE 2. Case studies of parallel-connected FoCs in (14)–(16).

$Z_{\text{eq,p}}(s)$ [Ω]	$\lvert Z_{\text{eq,p}}(s)\rvert$ [Ω]	$\text{Arg}[Z_{\text{eq,p}}(s)]$ [Degree]
Case III: $C_{\alpha_1} \neq C_{\alpha_2} \neq C_{\alpha_3} \neq \ldots \neq C_{\alpha_n}$ with identical order α		
$\frac{1}{s^\alpha\left(\sum_{i=1}^{n} C_{\alpha_i}\right)}$ (17)	$\frac{1}{\omega^\alpha\left(\sum_{i=1}^{n} C_{\alpha_i}\right)}$ (18)	$-\alpha\frac{\pi}{2}$ (19)
Case IV: $C_{\alpha_1} = C_{\alpha_2} = C_{\alpha_3} = \ldots = C_{\alpha_n} = C_\alpha$ with identical order α		
$\frac{1}{s^\alpha(nC_\alpha)}$ (20)	$\frac{1}{\omega^\alpha(nC_\alpha)}$ (21)	$-\alpha\frac{\pi}{2}$ (22)

III. EXPERIMENTAL VERIFICATION

A. BRIEF DISCUSSION ON AVAILABLE FoCs AND NEW DEVICES

Despite the significant demand for and importance of fractional-order capacitors in many applications listed above, the lack of commercial availability of FoCs and restricted realizations of their emulators discussed below limit the researchers in performing experimental tests and consequently the growth of this research area. In particular, only few works in open access literature report practical implementations of FoCs [32], [35]–[40]. The first attempt was based on the fabrication of an infinite ladder network [35], which later on continued by developing fractal structures on silicon [36], lithium ions on the rough surface of metal electrodes [37], using the electrolytic process [38], by dipping a capacitive-type polymer-coated probe in polarizable medium [39], or emulating the FoC behavior with OTA as an active building block [32], [40]. In general, however, the FoCs produced using these techniques operate properly only in a limited low frequency range of up to 1 MHz; they are bulky and not easy to reproduce with required specifications, or the phase error is higher than ± 5 degrees. Therefore, the phase response of FoC is not sufficiently stable and in specific frequency ranges significant ripples occur.

In this paper, three types of FoCs of different phase angles are fabricated [41], [42]. First, the PVDF and PVDF-TrFE-CFE powders are dissolved in a solvent, N, N-Dimethylformamide (DMF) separately in different vials (one vial for PVDF and three vials for PVDF-TrFE-CFE), under constant stirring at room temperature for two days to obtain 0.1 mg/ml polymer solutions. An rGO is weighed with the desired weight percentage, suspended in 1 ml DMF, and dispersed via ultrasonication for 1 hour. Later, dispersed rGO

TABLE 3. Measurement results of fabricated fractional-order capacitors (Note: * at $f_c = 2$ MHz).

Capacitor No.	Device Type	Device Pin No.	$\lvert Z\rvert^*$ [kΩ]	φ^* [Degree]	Order α^* [−]	Pseudo-Capacitance* [Farad·sec$^{\alpha-1}$]	Equivalent $C_{\text{int}}{}^*$ [F]	Phase Angle Deviation in Range (0.2–20) MHz [Degree]	Fabrication Technology
C_{α_1}	TP2	1	2.37	−61.91	0.69	5.52 n	33.6 p	±4.01	Polymer dielectric
C_{α_2}	TP2	4	2.24	−61.86	0.69	5.89 n	35.54 p	±3.84	Polymer dielectric
C_{α_3}	P2	9	6.09	−82.63	0.92	49.90 p	13.07 p	±3.18	Polymer dielectric
C_{α_4}	P2	8	6.43	−82.59	0.92	47.52 p	12.37 p	±3.12	Polymer dielectric
C_{α_5}	G2	1	1.64	−55.68	0.62	24.74 n	48.50 p	±3.15	rGO-Polymer Composite

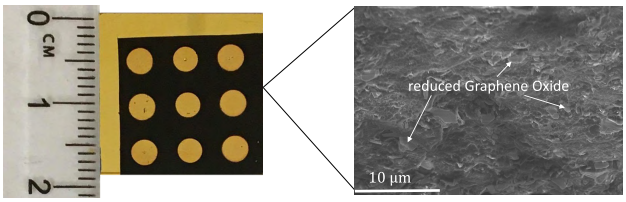

FIGURE 3. (a) 2 cm × 2 cm fabricated G2 device area with nine FoCs, (b) cross-sectional SEM image of rGO nanosheets/PVDF-TRFE-CFE nanocomposite, when the rGO nanosheets are distributed uniformly inside the polymer.

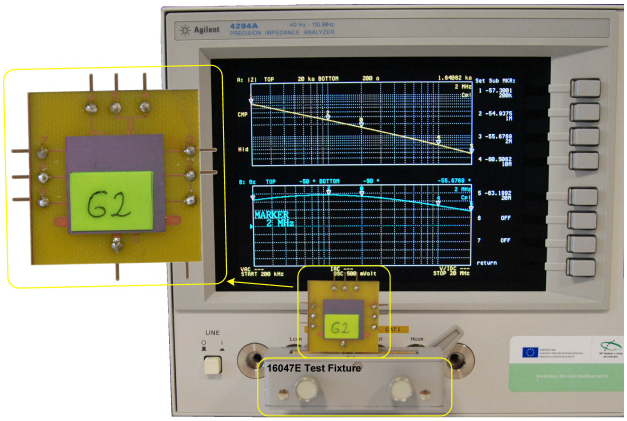

FIGURE 4. Experimental workstation and the fabricated solid-state G2 device (yellow line - impedance response; cyan-blue line - phase response).

solutions are poured onto the dissolved PVDF-TrFE-CFE (two vials) polymer solution and mixed under continuous stirring for another 24 hours. In total, three different polymer and composite solutions labeled TP2, P2, and G2 are prepared. Au-covered, 2 cm × 2 cm Si/Si_2 wafers are used to fabricate the FoC by drop-casting the composite solution. A 10 nm Ti layer followed by 190 nm Au layer is deposited on Si/SiO_2 wafers via DC sputter to define the bottom electrode. The composite solutions are drop-cast and dried for 12 hours at 85 °C under a vacuum. The other Au circular form electrodes of 3 mm diameter and 200 nm thickness are deposited in a similar way, using a shadow mask. Finally, nine samples of FoCs of the same order are flip-bonded on a printed circuit board and each capacitor gives a separate connection for the electrical measurements. The photo of an example of the fabricated G2 device, including a cross-sectional SEM image of rGO nanosheets/PVDF-TRFE-CFE nanocomposite, is shown in Fig. 3.

The behavior of three types (TP2, P2, G2) of fabricated FoCs of different orders (respectively $\alpha = 0.69, 0.92, 0.62$) was verified using the Agilent 4294A precision Impedance Analyzer. A photograph of the experimental workstation with fabricated solid-state G2 device is given in Fig. 4. During the experimental validation in the frequency range of our interest, 0.2 MHz − 20 MHz (801 logarithmically spaced points), a sinusoidal input signal with a default AC voltage of 500 mV and a frequency of 1 MHz was applied, while the common node was grounded ($V_g = 0$ V). Standard calibration tests (open and short circuits) of the 16047E Test Fixture were performed to calibrate the instrument. The measurement results are summarized in Table 3. Here, the magnitude, phase angle, i.e. FoC order, pseudo-capacitance, and equivalent integer-order capacitance at center frequency $f_c = 2$ MHz of the corresponding pins of all the devices are provided. From the results, a slight difference in the pseudo-capacitance values within the same device can be observed, which, however, gives us the flexibility to use different values within the same chip. On the other hand, the relative phase error at f_c is significantly low. In addition, the measured phase angle deviation in two decades of the frequency range of our interest is only ±4 degrees ([max − min]/2). Therefore, the main benefits of these fabricated devices against the above-discussed practical FoC realizations or emulators [32], [35]–[40] are that they demonstrate lower phase angle deviation, better tuning on phase angle, wider bandwidth, and reproducible results.

B. ARBITRARY-ORDER FoC CONNECTIONS

To validate the introduced theory, the series- and parallel-connected arbitrary-order FoC structures depicted in Figs. 1 and 2 and their selected interconnections were verified via experimental measurements using fabricated solid-state passive FoCs introduced above. The experimental setup described in Section III A was used. The magnitude and phase responses of equivalent FoCs obtained using the Agilent 4294A precision Impedance Analyzer were proved by theoretical calculations (values given in paren-

TABLE 4. Results of arbitrary-order series-connected two and three FoCs: Measurement (calculated via MATLAB code).

No.	#1	#2	#3	#4
Connection of FoCs	$C_{\alpha_1} + C_{\alpha_4}$	$C_{\alpha_1} + C_{\alpha_5}$	$C_{\alpha_4} + C_{\alpha_5}$	$C_{\alpha_1} + C_{\alpha_4} + C_{\alpha_5}$
Connection of Orders	$0.69 + 0.92$	$0.69 + 0.62$	$0.92 + 0.62$	$0.69 + 0.92 + 0.62$
Equivalent Impedance @ f_c [kΩ]	8.72 (8.51)	4.00 (3.82)	7.84 (7.73)	10.22 (9.83)
Phase [°]	−76.11 (−77.31)	−58.19 (−59.73)	−76.81 (−77.57)	−72.49 (−74.03)
Relative Phase Error [%]	−1.55	−2.58	−0.98	−2.08
Equivalent Order α [−]	0.85 (0.86)	0.65 (0.66)	0.85 (0.86)	0.81 (0.82)
Pseudo-Capacitance [Farad·sec$^{\alpha-1}$]	113.78 (93.72) p	6.42 (5.14) n	111.33 (98.47) p	187.33 (148.03) p

TABLE 5. Results of arbitrary-order parallel-connected two and three FoCs: Measurement (calculated via MATLAB code).

No.	#5	#6	#7	#8
Connection of FoCs	$C_{\alpha_1} \mid\mid C_{\alpha_4}$	$C_{\alpha_1} \mid\mid C_{\alpha_5}$	$C_{\alpha_4} \mid\mid C_{\alpha_5}$	$C_{\alpha_1} \mid\mid C_{\alpha_4} \mid\mid C_{\alpha_5}$
Connection of Orders	$0.69 \mid\mid 0.92$	$0.69 \mid\mid 0.62$	$0.92 \mid\mid 0.62$	$0.69 \mid\mid 0.92 \mid\mid 0.62$
Equivalent Impedance @ f_c [kΩ]	1.67 (1.72)	0.934 (0.934)	1.28 (1.27)	0.835 (0.812)
Phase [°]	−67.03 (−67.66)	−58.03 (−58.36)	−61.16 (−61.10)	−59.83 (−61.46)
Relative Phase Error [%]	−0.93	−0.57	0.10	−2.65
Equivalent Order α [−]	0.74 (0.75)	0.64 (0.65)	0.68 (0.68)	0.66 (0.68)
Pseudo-Capacitance [Farad·sec$^{\alpha-1}$]	3.10 (2.68) n	28.34 (26.67) n	11.66 (11.89) n	22.84 (17.42) n

TABLE 6. Results of interconnected (series-parallel) arbitrary-order FoCs: Measurement (calculated via MATLAB code).

No.	#9	#10
Connection of FoCs	$[(C_{\alpha_1} + C_{\alpha_2}) \mid\mid C_{\alpha_4}] + C_{\alpha_5}$	$C_{\alpha_1} \mid\mid C_{\alpha_4} \mid\mid (C_{\alpha_2} + C_{\alpha_3})$
Connection of Orders	$[(0.69 + 0.69) \mid\mid 0.92] + 0.62$	$0.69 \mid\mid 0.92 \mid\mid (0.69 + 0.92)$
Equivalent Impedance @ f_c [kΩ]	4.33 (4.26)	1.91 (1.39)
Phase [°]	−64.09 (−65.58)	−68.68 (−69.27)
Relative Phase Error [%]	−2.27	−0.85
Equivalent Order α [−]	0.71 (0.73)	0.76 (0.77)
Pseudo-Capacitance [Farad·sec$^{\alpha-1}$]	2.04 (1.58) n	2.01 (2.47) n

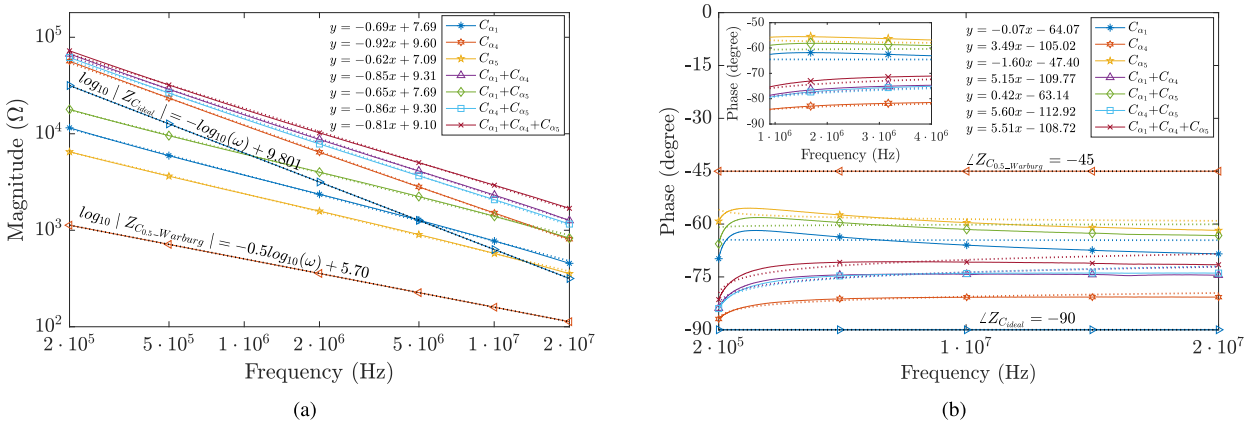

FIGURE 5. Two and three arbitrary-order FoCs connected in series: (a) magnitude, (b) phase responses.

theses in Tables 4–6) via the MATLAB open access source code given in Appendix. In order to compare the FoCs, the fundamental orders (the Warburg pseudo- and integer-order ideal capacitance are set as 790 nFarad·sec$^{-0.5}$ and 158 pF, respectively) are plotted in all Figures by means of magnitude and phase.

1) SERIES CONNECTION OF ARBITRARY-ORDER FoCs

Firstly, the magnitude and phase responses of two and three arbitrary-order series-connected FoCs were studied. The results obtained, including each individual FoC, are shown in Figs. 5(a) (magnitude) and (b) (phase), while the comparison of measured values at $f_c = 2$ MHz and calculated results is evaluated in Table 4. To estimate the equivalent order α (or phase), the magnitude data measured are fitted to the function $\log|Z| = \alpha \log f + \log(2\pi)^{\alpha} C_{\alpha}$ using the linear least squares (LLS) method. Note that the magnitude responses are given in the logarithmic scale, while the phase responses in linear scale. The equivalent equations from fitting the magnitude or phase as obtained from measurement

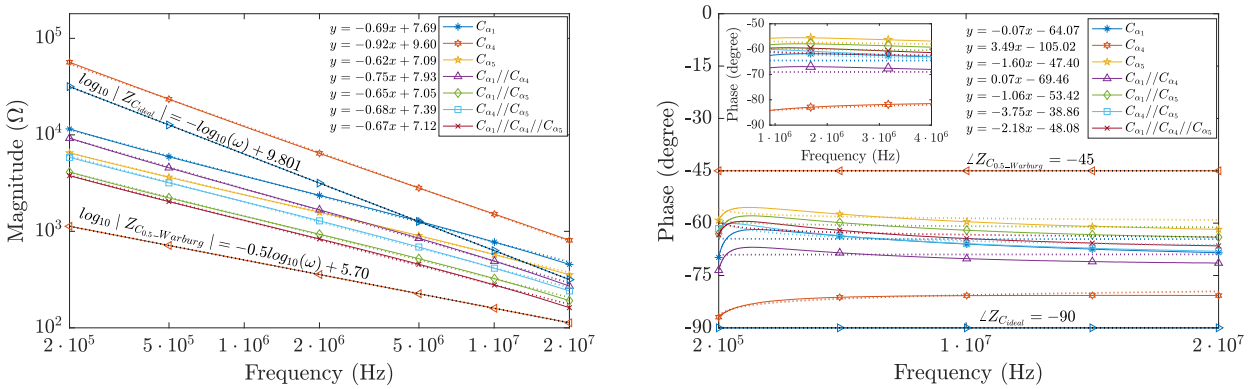

FIGURE 6. Two and three arbitrary-order FoCs connected in parallel: (a) magnitude, (b) phase responses.

samples are provided inside Fig. 5. From the results the orders are evident of FoCs as single devices TP2, P2, G2, i.e. 0.69, 0.92, and 0.62, with corresponding phases −61.91, −82.59, and −55.68 [degrees], while their equivalent orders from series connections are found to be 0.85, 0.65, 0.85, 0.81 (corresponding to Table 4 cases #1 → #4 with phases −76.11, −58.19, −76.81, −72.49). The equivalent magnitudes vary in ranges of (67.2 → 1.26, 17.87 → 0.829, 61.69 → 1.16, and 72.38 → 1.69) kΩ for cases #1 → #4, respectively. Via experiments we also demonstrated that the phase can be tuned by connecting different orders as depicted in Fig. 5(b). Furthermore, Table 4 gives the corresponding pseudo capacitances and relative phase errors of measured phases relative to the calculated values, which are at f_c in the range of −2.58% to −0.98%.

2) PARALLEL CONNECTION OF ARBITRARY-ORDER FoCs

Secondly, the behavior of two and three arbitrary-order FoCs connected in parallel were experimentally verified. The magnitude and phase responses of the equivalent impedances are shown in Figs. 6(a) and (b), respectively, while a comparison of the values measured at f_c and the results calculated via the MATLAB open access source code are listed in Table 5. The equivalent new orders, which are achieved using the LLS fitting and given in Fig. 6(a) next to the legend, are found to be 0.74, 0.64, 0.68, and 0.66. As can be observed, the orders match well to those obtained from the measured phase responses, which are depicted in Fig. 6(b). Overall, the equivalent impedances have capacitive behavior and vary in ranges of (9.24 → 0.27) kΩ, (4.11 → 0.19) kΩ, (5.84 → 0.24) kΩ, and (3.78 → 0.16) kΩ for cases #5 → #8, respectively. It is also worth noting that the relative phase errors at f_c are again small and vary in the range of −2.65% to 0.10%.

3) SERIES-PARALLEL INTERCONNECTION OF ARBITRARY-ORDER FoCs

Finally, two selected series-parallel interconnections of FoCs were evaluated. The equivalent impedance of the first topology from Fig. 7 can be expressed as:

$$Z_{\text{eq},\#9}(s) = \frac{3s^{\alpha_1}C_{\alpha_1} + 2s^{\alpha_4}C_{\alpha_4}}{s^{\alpha_1+\alpha_5}C_{\alpha_1}C_{\alpha_5} + 2s^{\alpha_4+\alpha_5}C_{\alpha_4}C_{\alpha_5}},\ [\Omega] \tag{23}$$

where $\alpha_1 \cong \alpha_2 \neq \alpha_4 \neq \alpha_5$ and $C_{\alpha_1} \cong C_{\alpha_2} \neq C_{\alpha_4} \neq C_{\alpha_5}$.

Similarly, the equivalent impedance of the structure given in Fig. 8 can be found as:

$$Z_{\text{eq},\#10}(s) = \frac{2}{2s^{\alpha_1}C_{\alpha_1} + 3s^{\alpha_3}C_{\alpha_3}},\ [\Omega] \tag{24}$$

while $\alpha_1 \cong \alpha_2 \neq \alpha_3 \cong \alpha_4$ and $C_{\alpha_1} \cong C_{\alpha_2} \neq C_{\alpha_3} \cong C_{\alpha_4}$.

Here it is important to note that this is the very first attempt in the literature to calculate and measure the equivalent magnitude and phase of the arbitrary-order interconnected FoCs. A detailed comparison of the results at f_c is given in Table 6 and depicted in Fig. 9. The equivalent orders of interconnections #9 and #10 obtained using the LLS fitting are 0.71 and 0.76, which correspond to the phases −64.09 and −68.68 [degrees], respectively. The calculated relative phase errors are respectively −2.27% and −0.85% for the first and second topology, which are very favorable results. Overall, from the results obtained it is clear that the measurement results are in very good agreement with theoretically predicted ones.

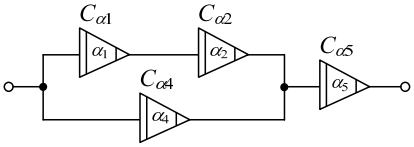

FIGURE 7. First series-parallel interconnection of arbitrary-order FoCs (#9).

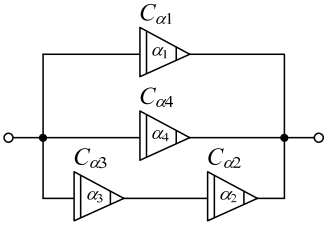

FIGURE 8. Second series-parallel interconnection of arbitrary-order FoCs (#10).

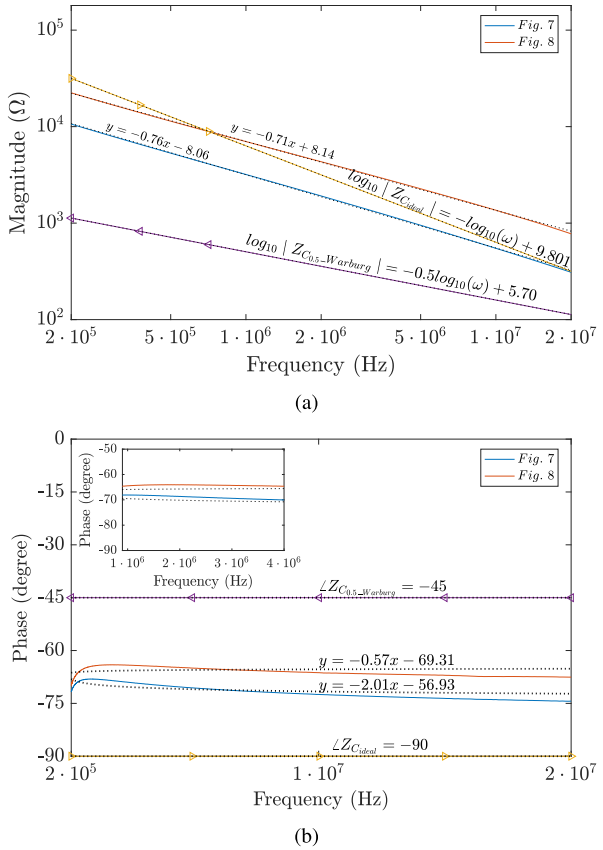

FIGURE 9. Interconnected FoCs given in Figs. 7 and 8: (a) magnitude, (b) phase responses.

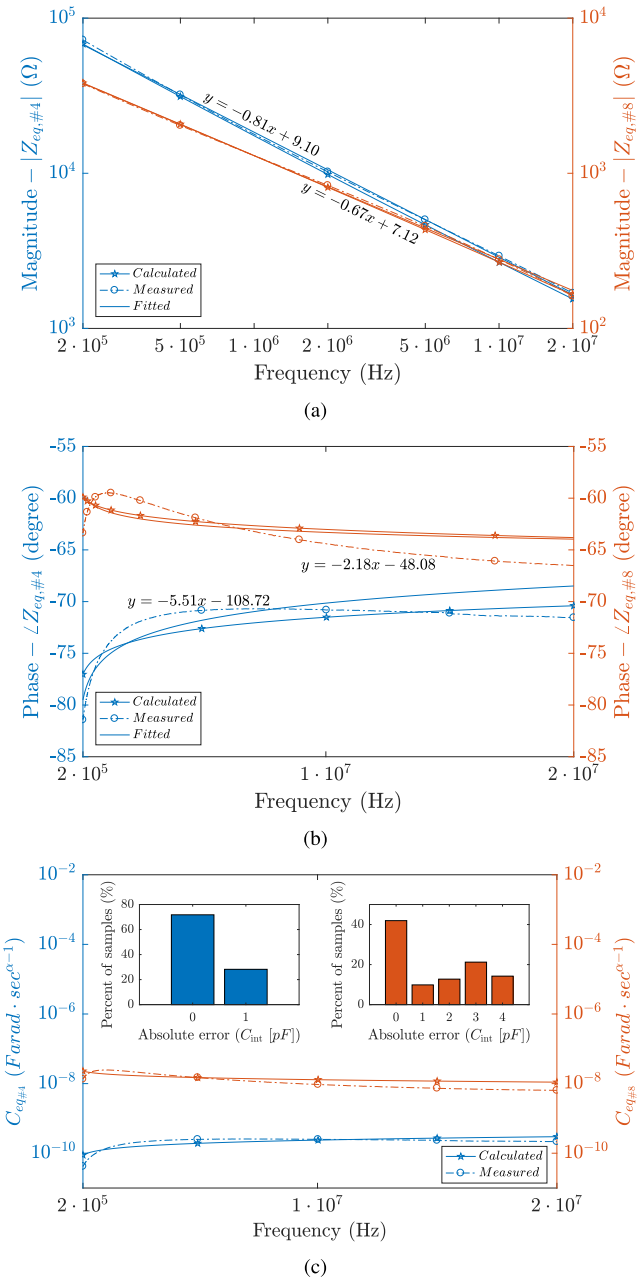

FIGURE 10. Comparison of (a) magnitude, (b) phase, and (c) pseudo-capacitance versus frequency of three arbitrary-order FoCs connected in series (#4 - blue color) and parallel (#8 - orange color).

IV. BRIEF DISCUSSION OF RESULTS

Figures 10(a) and (b) give a comparison of the calculated, measured, and fitted line values of the magnitude and phase responses of three arbitrary-order series- and parallel-connected FoCs (cases #4 and #8 of Tables 4 and 5, respectively). It is evident that the results calculated using the MATLAB open access source code match well with the fitted values and the measured values. Furthermore, the equivalent pseudo-capacitance versus frequency is plotted for both circuits in Fig. 10(c). As can be observed, the pseudo-capacitance of both FoCs is constant in the same region as the phase is. The normalized histograms show low absolute error between the measured and the calculated equivalent integer-order capacitance values, which is less than 1 pF and 4 pF, respectively, for the series- and parallel-connected FoCs.

Evaluating in brief the obtained results it can be concluded that the equivalent impedances of fabricated arbitrary-order FoCs connected in series and parallel exhibit the same capacitive behavior as integer-order capacitors. Despite the claim in [32], here it is important to underline that the phase responses of series- and parallel-connected FoCs of arbitrary orders are constant. The experimental results are in good agreement with theory and calculated results. Note that the accuracy of the above theoretical analyses is proved and the proposed approach offers flexibility and a degree of freedom to work with any order of FoCs with random connection.

V. CONCLUSION

The paper presented a novel analytical approach of series- and parallel-connected n arbitrary-order FoCs. Particularly, as practical case studies, two and three arbitrary-order FoCs were used in series- and parallel-connected circuits and the magnitude and phase responses, i.e. the order, of the equivalent impedances were evaluated in detail. In addition, the units of these physical dimensions were discussed. More-

Open access source code 1. MATLAB code for calculating equivalent FoCs.

```
%%%%%%%%%%%%%%%%%%%%%%%%%%%%%%%%%%%%%%%%%%%%%%%%%%%%%%%%%%%%%%%%%%%%%%%%
% MATLAB code for calculating the equivalent impedance of ...
      n FoCs and plotting the magnitude and phase responses
%
% Copyright (c) 2018, A. Kartci, A. Agambayev, N. ...
      Herencsar, and K.N. Salama
% Brno University of Technology & King Abdullah University ...
      of Science and Technology
% All rights reserved.
%
% Feel free to use/modify these codes as you see fit. Any ...
      publications codes, papers, technical reports, etc.) ...
      in which our codes (in their original or a modified ...
      format) have been used should cite the original paper.
%%%%%%%%%%%%%%%%%%%%%%%%%%%%%%%%%%%%%%%%%%%%%%%%%%%%%%%%%%%%%%%%%%%%%%%%

syms s f z z1

% Set the order and fractional-order capacitance value
order = [0.69 0.92 0.62];
FoC = [5.52e-9 47.52e-12 24.74e-9];

% Calculating the equivalent impedances
for n = 1:length(order)
  Z(n) = 1/((s^order(n))*FoC(n));
  pretty(Z(n));
  % Equivalent impedance of series connection
  Zstot = sum(Z(1:n));
  Y(n) = ((s^order(n))*FoC(n));
  pretty(Y(n));
  Zptot = sum(Y(1:n))
  % Equivalent impedance of parallel connection
  Zptot = 1/Zptot;
end

% Plotting the results for series-connected FoCs
NUM = eval(Zstot);
z = [z; (solve(NUM))];
zz = z/(2*pi);
f = logspace (2,7,1000);
l = size(f);
for n = 1:1:l(2)
% Magnitude of equivalent impendace (dB)
module(n) = (abs(subs(NUM,s,j*2*pi*f(n))));
end
for n = 1:1:l(2)
% Phase of equivalent impedance (degree)
phase(n) = (angle(subs(NUM,s,j*2*pi*f(n))))*180/pi;
end
figure(1);
subplot(2,1,1)
loglog(f,module,'-b','LineWidth',2)
hold on;
xlabel('Frequency (Hz)','FontSize',10)
ylabel('Magnitude (\Omega)','FontSize',10)
subplot(2,1,2)
semilogx(f,phase,'-b','LineWidth',2)
hold on;
xlabel('Frequency (Hz)','FontSize',10)
ylabel('Phase (degree)','FontSize',10)

% Plotting the results for parallel-connected FoCs
NUM1 = eval(Zptot);
z1 = [z1; (solve(NUM1))];
zz1 = z1/(2*pi);
f = logspace (2,7,1000);
l = size(f);
for n = 1:1:l(2)
% Magnitude of equivalent impendace (dB)
module1(n) = (abs(subs(NUM1,s,j*2*pi*f(n))));
end
for n = 1:1:l(2)
% Phase of equivalent impedance (degree)
phase1(n) = (angle(subs(NUM1,s,j*2*pi*f(n))))*180/pi;
end
figure(1);
subplot(2,1,1)
loglog(f,module1,'-.r','LineWidth',2)
hold on;
xlabel('Frequency (Hz)','FontSize',10)
ylabel('Magnitude (\Omega)','FontSize',10)
legend('Series connection', 'Parallel ...
      connection','Location','northeast');
subplot(2,1,2)
semilogx(f,phase1, '-.r','LineWidth',2)
hold off;
xlabel('Frequency (Hz)','FontSize',10)
ylabel('Phase (degree)','FontSize',10)
legend('Series connection', 'Parallel ...
      connection','Location','northeast');
```

over, the very first effort in the literature to derive and validate the equivalent magnitude and phase of arbitrary-order connected FoCs was successfully accomplished. The behavior of the equivalent FoCs was evaluated experimentally. During the measurements, three fabricated ferroelectric polymer and rGO-percolated P(VDF-TrFE-CFE) composite structure-based FoCs were used. In this regard, FoCs were found to be in orders of 0.69 for the first (TP2), 0.92 for the second (P2), and 0.62 for the third device (G2) over two decades, i.e. in the frequency range 0.2 MHz − 20 MHz. The obtained phase angle deviation of single devices at 2 MHz is ±4 degrees, while the calculated relative phase errors of all studied FoC connections at this frequency varied in a range of −2.65% to 0.10%. Furthermore, the enclosed MATLAB open access source code can be used as a powerful tool for precise calculation of any kind of series or parallel FoC connections based on their order and pseudo-capacitances.

APPENDIX

See Open access source code 1.

REFERENCES

[1] C.-C. Hu and T.-W. Tsou, "The optimization of specific capacitance of amorphous manganese oxide for electrochemical supercapacitors using experimental strategies," *Power Sources*, vol. 115, no. 1, pp. 179–186, 2003.

[2] H. J. In, S. Kumar, Y. Shao-Horn, and G. Barbastathis, "Origami fabrication of nanostructured, three-dimensional devices: Electrochemical capacitors with carbon electrodes," *Appl. Phys. Lett.*, vol. 88, no. 8, pp. 083104-1–083104-3, 2006.

[3] A. M. Elshurafa, M. N. Almadhoun, K. N. Salama, and H. N. Alshareef, "Microscale electrostatic fractional capacitors using reduced graphene oxide percolated polymer composites," *Appl. Phys. Lett.*, vol. 102, no. 23, pp. 232901-1–232901-4, 2013.

[4] N. Bertrand, J. Sabatier, O. Briat, and J. M. Vinassa, "Embedded fractional nonlinear supercapacitor model and its parametric estimation method," *IEEE Trans. Ind. Electron.*, vol. 57, no. 12, pp. 3991–4000, Dec. 2010.

[5] T. J. Freeborn, A. S. Elwakil, and B. J. Maundy, "Fractional-order models of supercapacitors, batteries and fuel cells: A survey," *Mater. Renew. Sustain. Energy*, vol. 4, p. 9, Sep. 2015.

[6] D. E. Shen, L. A. Estrada, A. M. Osterholm, D. H. Salazar, A. L. Dyer, and J. R. Reynolds, "Understanding the effects of electrochemical parameters on the areal capacitance of electroactive polymers," *Mater. Chem. A*, vol. 2, no. 20, pp. 7509–7516, 2014.

[7] R. R. Nigmatullin and S. O. Nelson, "Recognition of the 'fractional' kinetics in complex systems: Dielectric properties of fresh fruits and vegetables from 0.01 to 1.8 GHz," *Signal Process.*, vol. 86, no. 10, pp. 2744–2759, 2006.

[8] I. S. Jesus, J. A. T. Machado, and J. B. Cunha, "Fractional electrical impedances in botanical elements," *Vibrat. Control*, vol. 14, nos. 9–10, pp. 1389–1402, 2008.

[9] A. AboBakr, L. A. Said, A. H. Madian, A. S. Elwakil, and A. G. Radwan, "Experimental comparison of integer/fractional-order electrical models of plant," *AEU-Int. J. Electron. Commun.*, vol. 80, pp. 1–9, Oct. 2017.

[10] I. Podlubny, "Fractional-order systems and $PI^{\lambda}D^{\mu}$-controllers," *IEEE Trans. Autom. Control*, vol. 44, no. 1, pp. 208–213, Jan. 1999.

[11] R. Caponetto, G. Dongola, L. Fortuna, and I. Petras, *Fractional Order Systems: Modeling and Control Applications*, vol. 72. Singapore: World Scientific, 2010.

[12] Y. Luo and Y. Q. Chen, *Fractional Order Motion Control*. Hoboken, NJ, USA: Wiley, 2013.

[13] C. M. Ionescu and D. Copot, "Monitoring respiratory impedance by wearable sensor device: Protocol and methodology," *Biomed. Signal Process. Control*, vol. 36, pp. 57–62, Jul. 2017.

[14] A. Ates, B. B. Alagoz, G. Kavuran, and C. Yeroglu, "Implementation of fractional order filters discretized by modified fractional order darwinian particle swarm optimization," *Measurement*, vol. 107, pp. 153–164, Sep. 2017.
[15] A. G. Radwan, A. M. Soliman, and A. S. Elwakil, "First-order filters generalized to the fractional domain," *J. Circuits, Syst., Comput.*, vol. 17, no. 1, pp. 55–66, 2008.
[16] B. Maundy, A. S. Elwakil, and T. J. Freeborn, "On the practical realization of higher-order filters with fractional stepping," *Signal Process.*, vol. 91, no. 3, pp. 484–491, 2011.
[17] J. Jerabek *et al.*, "Reconfigurable fractional-order filter with electronically controllable slope of attenuation, pole frequency and type of approximation," *J. Circuits, Syst. Comput.*, vol. 26, no. 10, pp. 1750157-1–1750157-21, 2017.
[18] G. Tsirimokou, C. Psychalinos, A. S. Elwakil, and K. N. Salama, "Electronically tunable fully integrated fractional-order resonator," *IEEE Trans. Circuits Syst. II, Exp. Briefs*, vol. 65, no. 2, pp. 166–170, Feb. 2018.
[19] A. G. Radwan, A. S. Elwakil, and A. M. Soliman, "Fractional-order sinusoidal oscillators: Design procedure and practical examples," *IEEE Trans. Circuits Syst. I, Reg. Papers*, vol. 55, no. 7, pp. 2051–2063, Aug. 2008.
[20] A. Kartci *et al.*, "Fractional-order oscillator design using unity-gain voltage buffers and OTAs," in *Proc. 60th IEEE Int. Midwest Symp. Circuits Syst. (MWSCAS)*, Boston, MA, USA, Aug. 2017, pp. 555–558.
[21] A. S. Elwakil, A. Agambayev, A. Allagui, and K. N. Salama, "Experimental demonstration of fractional-order oscillators of orders 2.6 and 2.7," *Chaos, Solitons Fractals*, vol. 96, pp. 160–164, Mar. 2017.
[22] A. G. Radwan and K. N. Salama, "Passive and active elements using fractional $L_\beta C_\alpha$ circuit," *IEEE Trans. Circuits Syst. I, Reg. Papers*, vol. 58, no. 10, pp. 2388–2397, Oct. 2011.
[23] Y. Shang, H. Yu, and W. Fei, "Design and analysis of CMOS-based terahertz integrated circuits by causal fractional-order RLGC transmission line model," *IEEE J. Emerg. Sel. Topics Circuits Syst.*, vol. 3, no. 3, pp. 355–366, Sep. 2013.
[24] K. Rajagopal, A. Karthikeyan, and P. Duraisamy, "Hyperchaotic chameleon: Fractional order FPGA implementation," *Complexity*, vol. 2017, May 2017, Art. no. 8979408.
[25] J. L. Adams, A. Madanayake, and L. T. Bruton, "Approximate realization of fractional-order 2-D IIR frequency-planar filters," *IEEE J. Emerg. Sel. Topics Circuits Syst.*, vol. 3, no. 3, pp. 338–345, Mar. 2013.
[26] Y.-F. Pu, "Analog circuit realization of arbitrary-order fractional hopfield neural networks: A novel application of fractor to defense against chip cloning attacks," *IEEE Access*, vol. 4, pp. 5417–5435, 2016.
[27] S. Westerlund and L. Ekstam, "Capacitor theory," *IEEE Trans. Dielectr. Electr. Insul.*, vol. 1, no. 5, pp. 826–839, Oct. 1994.
[28] Y. Zhang *et al.*, "Excellent dielectric properties of anisotropic polymer composites filled with parallel aligned zinc flakes," *Appl. Phys. Lett.*, vol. 101, no. 19, pp. 192904-1–192904-4, 2012.
[29] T. J. Freeborn, B. Maundy, and A. S. Elwakil, "Measurement of supercapacitor fractional-order model parameters from voltage-excited step response," *IEEE J. Emerging Sel. Topics Circuits Syst.*, vol. 3, no. 3, pp. 367–376, Sep. 2013.
[30] A. Allagui, A. S. Elwakil, B. J. Maundy, and T. J. Freeborn, "Spectral capacitance of series and parallel combinations of supercapacitors," *ChemElectroChem*, vol. 3, no. 9, pp. 1429–1436.
[31] F. Wang and X. Ma, "Analysis of fractional order capacitor in series and parallel connections," *Chinese Science Paper Online*, pp. 1–8, 2013.
[32] G. Tsirimokou, C. Psychalinos, A. S. Elwakil, and K. N. Salama, "Experimental behavior evaluation of series and parallel connected constant phase elements," *AEU-Int. J. Electron. Commun.*, vol. 74, pp. 5–12, Apr. 2017.
[33] Y.-F. Pu, "Measurement units and physical dimensions of fractance—Part I: Position of purely ideal fractor in Chua's axiomatic circuit element system and fractional-order reactance of fractor in its natural implementation," *IEEE Access*, vol. 4, pp. 3379–3397, 2016.
[34] Y.-F. Pu, "Measurement units and physical dimensions of fractance—Part II: Fractional-order measurement units and physical dimensions of fractance and rules for fractors in series and parallel," *IEEE Access*, vol. 4, pp. 3398–3416, 2016.
[35] S. D. Roy, "On the realization of a constant-argument immittance or fractional operator," *IEEE Trans. Circuit Theory*, vol. CT-14, no. 3, pp. 264–274, Sep. 1967.
[36] T. C. Haba, G. Ablart, T. Camps, and F. Olivie, "Influence of the electrical parameters on the input impedance of a fractal structure realised on silicon," *Chaos, Solitons Fractals*, vol. 24, no. 2, pp. 479–490, 2005.
[37] G. W. Bohannan, "Analog fractional order controller in temperature and motor control applications," *J. Vibrat. Control*, vol. 14, nos. 9–10, pp. 1487–1498, 2008.
[38] I. S. Jesus and J. A. T. Machado, "Development of fractional order capacitors based on electrolyte processes," *Nonlinear Dyn.*, vol. 56, no. 1, pp. 45–55, Apr. 2009.
[39] K. Biswas, S. Sen, and P. K. Dutta, "Realization of a constant phase element and its performance study in a differentiator circuit," *IEEE Trans. Circuits Syst. II, Exp. Briefs*, vol. 53, no. 9, pp. 802–806, Sep. 2006.
[40] G. Tsirimokou, C. Psychalinos, A. S. Elwakil, and K. N. Salama, "Experimental verification of on-chip CMOS fractional-order capacitor emulators," *Electron. Lett.*, vol. 52, no. 15, pp. 1298–1300, Jul. 2016.
[41] A. Agambayev, S. Patole, M. Farhat, A. Elwakil, H. Bagci, and K. N. Salama, "Ferroelectric fractional-order capacitors," *ChemElectroChem*, vol. 4, no. 11, pp. 2807–2813, 2017.
[42] A. Agambayev, S. Patole, H. Bagci, and K. N. Salama, "Tunable fractional-order capacitor using layered ferroelectric polymers," *AIP Adv.*, vol. 7, no. 9, pp. 095202-1–095202-8, 2017.

ASLIHAN KARTCI (S'15) received the M.S. degree in electronics from Yildiz Technical University, Turkey, in 2015. She is currently pursuing the Ph.D. degree with the Department of Radio Electronics, Brno University of Technology, Czech Republic. Her research interests include fractional-order analog integrated circuits with modern active elements and their application as oscillators and filters, general element simulator, numerical methods for analysis of electronic networks, and computer-aided methods for the simulation of electronic circuits for high-frequency applications.

AGAMYRAT AGAMBAYEV (S'15) was born in Mary, Turkmenistan, in 1992. He received the B.S. degree in physics with double majoring in electrical and electronics engineering and the M.S. degree in biomedical engineering from Fatih University, Istanbul, Turkey, in 2012 and 2014, respectively. He is currently pursuing the Ph.D. degree in electrical engineering with the King Abdullah University of Science and Technology, Thuwal, Saudi Arabia. His research interests include modeling, designing, and application of the fractional-order circuit elements and nanocomposites for energy storage systems.

NORBERT HERENCSAR (S'07–M'12–SM'15) received the M.S. degree in electronics and communication and the Ph.D. degree in teleinformatics from the Brno University of Technology (BUT), Brno, Czech Republic, in 2006 and 2010, respectively.

In 2013 and 2014, he was a Visiting Researcher with Bogazici University, Istanbul, Turkey, and Dogus University, Istanbul. Since 2006, he has been collaborating on numerous research projects supported by the Czech Science Foundation. Since 2015, he has been an Associate Professor with the Department of Telecommunications, BUT. He is currently an MC Member of the COST Action CA15225. He has authored 72 articles published in SCI-E peer-reviewed journals and about 110 papers published in the proceedings of international conferences. His research interests include analog electronics, current-mode circuits, and fractional-order systems synthesis.

Dr. Herencsar is also a Senior Member of the IACSIT and IRED and a member of the IAENG, ACEEE, and RS. He has been the Deputy Chair of the International Conference on Telecommunications and Signal Processing (TSP) and an Organizing or TPC Member of the AFRICON, ELECO, I^2MTC, ICUMT, IWSSIP, SET-CAS, MWSCAS, and ICECS conferences since 2010. In 2016, he was the General Co-Chair of the COST/IEEE-CASS Seasonal Training School in Fractional-Order Systems. Since 2017, he has been the General Co-Chair of the TSP. Since 2011, he has been a Guest Co-Editor to several special journal issues in *AEU–International Journal of Electronics and Communications, Radioengineering, and Telecommunication Systems*. Since 2014 and 2017, he has been serving as an Associate Editor of the *Journal of Circuits, Systems and Computers* and the IEEE Access, respectively. Since 2015, he has been serving with the IEEE Czechoslovakia Section Executive Committee as the SP/CAS/COM Joint Chapter Chair and a Membership Development Officer.

KHALED N. SALAMA (S'97–M'05–SM'10) received the B.S. degree (Hons.) from the Department of Electronics and Communications, Cairo University, Cairo, Egypt, in 1997, and the M.S. and Ph.D. degrees from the Department of Electrical Engineering, Stanford University, Stanford, CA, USA, in 2000 and 2005, respectively.

He was an Assistant Professor with the Rensselaer Polytechnic Institute, Troy, NY, USA, from 2005 to 2009. In 2009, he joined the King Abdullah University of Science and Technology, Saudi Arabia, where he is currently an Associate Professor and was also the founding Program Chair until 2011. His work on CMOS sensors for molecular detection has been funded by the National Institutes of Health and the Defense Advanced Research Projects Agency, received the Stanford-Berkeley Innovators Challenge Award in biological sciences and was acquired by Lumina Inc. He has authored 150 papers and 14 patents on low-power mixed signal circuits for intelligent fully integrated sensors and nonlinear electronics, in particular memristor devices.